Available online at www.sciencedirect.com
ScienceDirect
International Journal of Mechanical Sciences 48 (2006) 1197–1207
International Journal of MECHANICAL SCIENCES
www.elsevier.com/locate/ijmecsci

Deformation and bifurcation analysis of boron-nitride nanotubes

J. Song[a], Y. Huang[a,*], H. Jiang[b], K.C. Hwang[c], M.F. Yu[a]

[a]Department of Mechanical Science and Engineering, University of Illinois, 1206 W. Green Street, Urbana, IL 61801, USA
[b]Department of Mechanical and Aerospace Engineering, Arizona State University, Tempe, Arizona 85287-6106, USA
[c]Department of Engineering Mechanics, Tsinghua University, Beijing 100084, China

Received 14 October 2005; received in revised form 21 February 2006; accepted 22 June 2006
Available online 7 August 2006

Abstract

Boron-nitride nanotubes (BNNTs) display unique properties and have many potential applications. An atomistic-based continuum theory is developed for BNNTs. The continuum constitutive model for BNNTs is obtained directly from interatomic potentials for boron and nitrogen. Such an approach involves no additional fitting parameters beyond those introduced in interatomic potentials. The atomistic-based continuum theory is then applied to study the Young's modulus, stress–strain curve and nonlinear bifurcation in BNNTs. It is shown that the mechanical behavior of BNNTs is virtually independent of the diameter and length of BNNTs, but has a strong dependence on helicity.

Keywords: Boron-nitride nanotube; Continuum analysis; Interatomic potential

1. Introduction

Boron-nitride nanotubes (BNNTs) represent an important class of nanotube since they possess unique structural, mechanical, thermal, electrical and chemical properties. For example, zigzag BNNTs are preferred over armchair and chiral BNNTs when grown by chemical vapor deposition at certain conditions [1]. The Young's modulus of BNNTs is on the order of 1TPa [2,3], and is comparable to that of carbon nanotubes. The thermal conductivity along the nanotube is also very high. However, contrary to carbon nanotubes, BNNTs always have large band gaps regardless of the chirality and diameter, and are therefore semiconductors. They also have good resistance to oxidation at high temperature.

There are very limited experimental [4,5] and atomistic studies e.g. [2,3,6–11] on the mechanical properties of BNNTs. The purpose of the present paper is to establish a continuum theory for BNNTs based on interatomic potentials for boron and nitrogen [12,13]. Similar to [14,15,28,33] studies of carbon nanotubes, this atomistic-based contunuum theory is established by modifying the Cauchy–Born rule for BNNTs to ensure the equilibrium of boron and nitrogen atoms. The continuum constitutive model is established directly from the atomic structure of BNNTs and interatomic potentials for boron and nitrogen. We then study the Young's modulus, stress–strain curve and nonlinear bifurcation of BNNTs.

This paper is structured as follows. The interatomic potential for boron and nitrogen is summarized in Section 2. This potential is used to establish a continuum constitutive model for BNNTs via the modified Cauchy–Born rule in Section 3. The Young's modulus and stress–strain curve given by this atomistic-based continuum theory are shown in Section 4. Section 5 gives the equilibrium equation for BNNTs, while the bifurcation analysis is presented in Section 6.

2. An interatomic potential for boron nitride

[13] established an interatomic potential for boron nitride as

$$V(r_{ij};\theta_{ijk}) = V_R(r_{ij}) - B_{ij}V_A(r_{ij}), \tag{1}$$

where V_R and V_A are the repulsive and attractive pair terms that depend only on the distance r_{ij} between a pair of atoms

*Corresponding author. Tel.: +1 217 265 5072; fax: +1 217 244 6534.
E-mail address: huang9@uiuc.edu (Y. Huang).

0020-7403/$ - see front matter © 2006 Elsevier Ltd. All rights reserved.
doi:10.1016/j.ijmecsci.2006.06.006

i and j, and are given by

$$V_R(r) = \frac{D_0}{S-1}\exp\left[-\beta\sqrt{2S}(r-r_0)\right]\cdot f_C(r),$$
$$V_A(r) = \frac{SD_0}{S-1}\exp\left[-\beta\sqrt{2/S}(r-r_0)\right]\cdot f_C(r), \quad (2)$$

D_0 and r_0 are the dimmer energy and separation, respectively, and they are given in Table 1 together with constants S and β. It is important to note that these constants depend on the index pair, i.e., they take different values for boron–nitrogen, nitrogen–nitrogen, and boron–boron atomistic interactions. The cutoff function f_C in (2) limits the interaction shell on the next neighbors inside the radius R, and is given by

$$f_C(r) = \begin{cases} 1, & r \leqslant R-D, \\ \frac{1}{2}-\frac{1}{2}\sin\left[(\pi r - R)/(2D)\right], & |r-R| \leqslant D, \\ 0, & r \geqslant R+D, \end{cases} \quad (3)$$

where $R = 2A$ and $D = 0.1A$ for all index pairs (i.e., for all boron–nitrogen, nitrogen–nitrogen and boron–boron atomistic interactions) as shown in Table 1. The interatomic potential in (1) also depends on the bond angle θ_{ijk} via the multi-body coupling term B_{ij}, which results from the interaction between atoms i,j and their local environment, and is given by

$$B_{ij} = \left(1+\gamma^n\chi_{ij}^n\right)^{-1/(2n)},$$
$$\chi_{ij} = \sum_{k\neq i,j} G(\theta_{ijk}) f_C(r_{ik}) \exp\left[\lambda^3\left(r_{ij}-r_{ik}\right)^3\right],$$
$$G(\theta_{ijk}) = 1 + \frac{c^2}{d^2} - \frac{c^2}{d^2+\left(h-\cos\theta_{ijk}\right)^2}, \quad (4)$$

where k denotes atoms other than i and j, r_{ik} is the distance between atoms i and k, f_C is the cutoff function in (3), θ_{ijk} denotes the angle between bonds i–j and i–k. The constants n, γ, λ, c, d and h depend on the index pair ij, as shown in Table 1.

We have verified that the interatomic potential given above does give the correct lattice constants for cubic boron-nitride and hexagonal boron-nitride atomic structures (e.g., [16–18]). Albe and Möller [12], Koga et al. [19], and Sibona et al. [20] used this interatomic potential to investigate boron-nitride thin film growth, ion bombardment in boron-nitride thin film deposition, and boron-nitride layered materials, respectively. [10,21] investigated the structural/thermal behavior of and defect formation in BNNTs.

Table 1
Parameters in the boron-nitride interatomic potential [12,13]

	BN-interaction	NN-interaction	BB-interaction
D_0(eV)	6.36	9.91	3.08
$r_0(A)$	1.33	1.11	1.59
S	1.0769	1.0769	1.0769
$\beta(A^{-1})$	2.043057	1.92787	1.5244506
$R(A)$	2.0	2.0	2.0
$D(A)$	0.1	0.1	0.1
n	0.364153367	0.6184432	3.9929061
γ	0.000011134	0.019251	0.0000016
$\lambda(A^{-1})$	1.9925	0	0
c	1092.9287	17.7959	0.52629
d	12.38	5.9484	0.001587
h	−0.5413	0	0.5

3. An atomistic-based constitutive model for boron-nitride nanotubes

3.1. Single-wall boron-nitride nanotubes prior to deformation

Fig. 1a shows a schematic diagram of a boron-nitride nanotube prior to deformation. Unlike a carbon nanotube that all carbon atoms are on the same cylindrical surface, there exists a certain degree of buckling with boron atoms displaced toward the tube axis and nitrogen atoms pushed outwards [2,3,6]. Let d_t and $d_t-2\Delta r$ denote the diameters of cylinders for nitrogen atoms and boron atoms, respectively, where Δr is the difference in radii of nitrogen and boron atoms to the nanotube axis.

We extend [15] method for carbon nanotubes to BNNT by mapping the BNNT in Fig. 1a to a two dimensional planar sheet in Fig. 1b, in which A, E and F denote boron atoms and B, C and D denote nitrogen atoms. This can be visualized by mapping radially the boron atoms onto the cylindrical surface of nitrogen atoms, then cutting this cylindrical surface (of nitrogen atoms) along its axial direction and unrolling it to a plane without stretching.

Fig. 1c shows a representative unit cell of the "unrolled" plane. Let $\boldsymbol{a}_1$ and $\boldsymbol{a}_2$ denote the vectors $\overrightarrow{BC}$ and $\overrightarrow{DC}$, respectively, and a_1 and a_2 be corresponding lengths. The length of BD is denoted by a_3 and the lengths of AB and AC are denoted by a_4 and a_5, respectively. Other lengths and angles in the 2D plane are completely determined by $a_1, a_2, \ldots, a_5$. For example, $\varphi_1 = \angle CBD$, $\varphi_2 = \angle CBA$, length of AD a_6, and $\varphi_3 = \angle BAD$ are given in terms of a_i $(i = 1, 2, \ldots, 5)$ by

$$\varphi_1 = \cos^{-1}\frac{a_1^2+a_3^2-a_2^2}{2a_1a_3},$$
$$\varphi_2 = \cos^{-1}\frac{a_1^2+a_4^2-a_5^2}{2a_1a_4},$$
$$a_6 = \sqrt{a_3^2+a_4^2-2a_3a_4\cos(\varphi_1-\varphi_2)},$$
$$\varphi_3 = \cos^{-1}\frac{a_4^2+a_6^2-a_3^2}{2a_4a_6}. \quad (5)$$

Fig. 1c also shows the chiral vector C_h which denotes the circumferential direction of the BNNT on this "unrolled" plane. The chiral vector can always be expressed in terms of the base vectors $\boldsymbol{a}_1$ and $\boldsymbol{a}_2$ as

$$\boldsymbol{C}_h = n\boldsymbol{a}_1 + m\boldsymbol{a}_2, \quad (6)$$

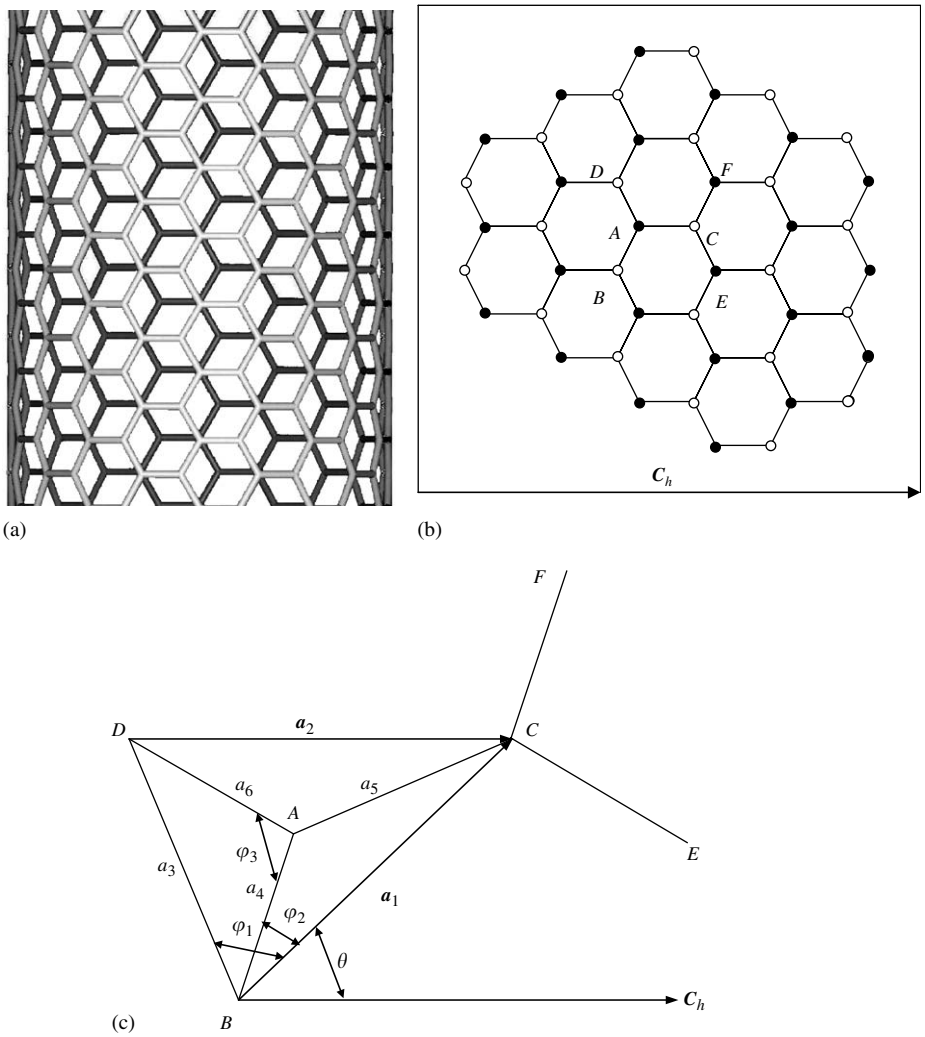

Fig. 1. A boron-nitride nanotube (BNNT) prior to deformation: (a) a schematic diagram of BNNT; (b) a planar, "unrolled" BNNT; the solid circles represent boron atoms, and open circles represent nitrogen atoms; and (c) a representative unit cell of the planar BNNT.

where n and m are integers, $n \geqslant m \geqslant 0$, and the pair (n, m) is called the chirality of the BNNT; $(n, 0)$ and (n, n) are called zigzag and armchair BNNTs, respectively, while $n > m > 0$ is called a chiral BNNT. Using the fact $\boldsymbol{a}_1 \cdot \boldsymbol{a}_1 = a_1^2$, $\boldsymbol{a}_2 \cdot \boldsymbol{a}_2 = a_2^2$ and $2\boldsymbol{a}_1 \cdot \boldsymbol{a}_2 = a_1^2 + a_2^2 - a_3^2$, we find

$$|\boldsymbol{C}_h| = \sqrt{\boldsymbol{C}_h \cdot \boldsymbol{C}_h} = \sqrt{n^2 a_1^2 + m^2 a_2^2 + mn(a_1^2 + a_2^2 - a_3^2)}. \tag{7}$$

This gives the diameter of the cylinder of the nitrogen atoms as $d_t = |\boldsymbol{C}_h|/\pi$. The angle between $\boldsymbol{C}_h$ and $\overrightarrow{BC}$ is denoted by θ, and is given by

$$\theta = \cos^{-1} \frac{\boldsymbol{C}_h \cdot \boldsymbol{a}_1}{|\boldsymbol{C}_h| a_1} = \cos^{-1} \frac{n a_1^2 + m/2(a_1^2 + a_2^2 - a_3^2)}{|\boldsymbol{C}_h| a_1}. \tag{8}$$

It is important to note that the bond length and angle used to calculate the energy stored in an atomic bond should be evaluated for the cylindrical configuration of BNNT (Fig. 1a), not the 2D planar one (Fig. 1b). In the following we obtain the cylindrical coordinates (R, Θ, Z) for atoms A, B, C, D, E and F in terms of a_i $(i = 1,2,\ldots 5)$ and Δr. It is obvious that

$$\begin{aligned} R_A &= R_E = R_F = d_t/2 - \Delta r, \\ R_B &= R_C = R_D = d_t/2. \end{aligned} \tag{9}$$

Without losing generality, we may take the polar angle Θ_B and axial coordinate Z_B of atom B as zero, i.e., $\Theta_B = Z_B = 0$. The axial and polar coordinates of atoms A, C, D, E and F are given by

$$\begin{aligned} Z_A &= a_4 \sin(\varphi_2 + \theta), \\ Z_C &= a_1 \sin\theta, \\ Z_D &= a_3 \sin(\varphi_1 + \theta), \\ Z_E &= a_1 \sin\theta - a_6 \sin(\varphi_3 - \varphi_2 - \theta), \\ Z_F &= a_1 \sin\theta + a_4 \sin(\varphi_2 + \theta), \end{aligned} \tag{10}$$

and

$$\Theta_A = \frac{2a_4\cos(\varphi_2+\theta)}{d_t},$$
$$\Theta_C = \frac{2a_1\cos\theta}{d_t},$$
$$\Theta_D = \frac{2a_3\cos(\varphi_1+\theta)}{d_t},$$
$$\Theta_E = \frac{2a_1\cos\theta+2a_6\cos(\varphi_3-\varphi_2-\theta)}{d_t},$$
$$\Theta_F = \frac{2a_1\cos\theta+2a_4\cos(\varphi_2+\theta)}{d_t}. \quad (11)$$

The bond length between two atoms X and Y ($X, Y = A, B, C, D, E, F$) with coordinates (R_X, Θ_X, Z_X) and (R_Y, Θ_Y, Z_Y) is given by

$$r_{XY} = \sqrt{(R_X\cos\Theta_X - R_Y\cos\Theta_Y)^2 + (R_X\sin\Theta_X - R_Y\sin\Theta_Y)^2 + (Z_Y - Z_X)^2}. \quad (12)$$

Once all bond lengths are known, the bond angle θ_{XYQ} can be obtained (where Q represents neighbor atoms). For a given chirality (n, m) of the BNNT, the bond length in (12) as well as the energy $V(r_{XY}; \theta_{XYQ})$ stored in bond XY are functions of a_i ($i = 1,2,\ldots,5$) and Δr. The energy W per unit cell is

$$W(a_1,a_2,a_3,a_4,a_5,\Delta r) = W_{boron} + W_{nitrogen},$$
$$W_{boron} = \left[V(r_{AB};\theta_{ABQ}) + V(r_{AC};\theta_{ACQ}) + V(r_{AD};\theta_{ADQ})\right]/2,$$
$$W_{nitrogen} = \left[V(r_{CA};\theta_{CAQ}) + V(r_{CE};\theta_{CEQ}) + V(r_{CF};\theta_{CFQ})\right]/2 \quad (13)$$

where W_{boron} and $W_{nitrogen}$ are the energy per boron and nitrogen atom. The lengths a_i ($i = 1,2,\ldots,5$) and Δr can be determined from energy minimization

$$\begin{cases} \dfrac{\partial W}{\partial a_i} = 0, \quad i = 1,2,\cdots,5, \\ \dfrac{\partial W}{\partial \Delta r} = 0, \end{cases} \quad (14)$$

Table 2 shows the diameter, bond lengths and bond angles of different BNNTs obtained from the above analysis. The results agree well with atomistic calculations [2,3,6,22] also shown in Table 2. Table 2 also shows the present analysis gives a vanishing Δr, while that obtained by atomistic calculations is not zero but extremely small (around 0.005 nm). In fact, we have used molecular mechanics based on the same interatomic potential [13] given in Section 2, and the molecular mechanics calculation indeed gives vanishing Δr prior to deformation as well as in simple tension. Therefore, the energy W_{boron} is the same as $W_{nitrogen}$ such that we can use a boron atom A and three nitrogen atoms B, C and D to calculate the strain energy density in the following sections.

3.2. Continuum description of deformed single-wall boron-nitride nanotube

The continuum deformation measures of deformed BNNTs can be related to the motion of many atoms via the Cauchy–Born rule [23,24]. The Cauchy—Born rule equates the strain energy at continuum level to the energy stored in atomic bonds. It also states that atoms subject to a homogeneous deformation move according to a single mapping from the undeformed to deformed configurations. From the continuum level, this mapping is taken to be the deformation gradient $\boldsymbol{F} = \partial\boldsymbol{x}/\partial\boldsymbol{X}$, where $\boldsymbol{X}$ and $\boldsymbol{x}$ denote positions of a material point in the undeformed and deformed configurations, respectively. A bond between a pair of atoms i and j in the undeformed configuration is described by a vector $\boldsymbol{r}_{ij}^{(0)}$. Upon deformation, the bond is described by

$$\boldsymbol{r}_{ij} = \boldsymbol{F}\cdot\boldsymbol{r}_{ij}^{(0)}, \quad (15)$$

and its length becomes

$$r_{ij} = \sqrt{\boldsymbol{r}_{ij}\cdot\boldsymbol{r}_{ij}} = \sqrt{\boldsymbol{r}_{ij}^{(0)}\cdot(\boldsymbol{I}+2\boldsymbol{E})\cdot\boldsymbol{r}_{ij}^{(0)}}, \quad (16)$$

where $\boldsymbol{E} = \frac{1}{2}(\boldsymbol{F}^T\cdot\boldsymbol{F} - \boldsymbol{I})$ is the Green strain tensor and $\boldsymbol{I}$ is the second-order identity tensor. For a centrosymmetric lattice structure that has pair of bonds in the opposite directions ($\boldsymbol{r}$ and $-\boldsymbol{r}$) around each atom, the Cauchy—Born rule ensures equilibrium of atoms because forces in the opposite, centrosymmetric bonds are always equal and opposite for arbitrarily imposed homogeneous deformation.

The Cauchy—Born rule cannot be applied to BNNTs because they do not have a centrosymmetric lattice structure such that the Cauchy—Born rule cannot ensure equilibrium of atoms anymore. Modifications of the Cauchy—Born rule for non-centrosymmetric lattice structures have been proposed [15,25–28]. For example [15] modified the Cauchy—Born rule to study carbon nanotubes, which have the same atomic structure as BNNTs except that all boron and nitrogen atoms are replaced by carbon atoms. [15] showed that a carbon nanotube subject to tension E_{ZZ} along the tube axis in the cylindrical configuration is equivalent to imposing the strain $E_{22} = E_{ZZ}$ in the unrolled plane followed by rolling the deformed, "unrolled" plane back to a tube. Here E_{22} denotes the strain normal to $\boldsymbol{C}_h$ direction in the "unrolled" plane.

We follow [15] approach in the present study of BNNTs. Fig. 2 shows the plane "unrolled" from a deformed BNNT.

Table 2
Structure of single wall BNNT prior to deformation

	Chirality (n,m)	Diameter d_t (nm)	Bond lengths (nm)			Bond angles (degree)			$\Delta r = R_N - R_B$ (nm)
			$r_{AB}^{(0)}$	$r_{AC}^{(0)}$	$r_{AD}^{(0)}$	$\angle BAC^{(0)}$	$\angle BAD^{(0)}$	$\angle CAD^{(0)}$	
Flat	$n+m \to \infty$	∞	0.14623	0.14623	0.14623	120	120	120	
			(0.1446)[c]	(0.1446)[c]	(0.1446)[c]	(120)[c]	(120)[c]	(120)[c]	
Zigzag	(6,0)	0.50242	0.14718	0.14718	0.14718	117.171	117.930	117.930	0
		(0.497)[c]	(0.1454)[c]	(0.1454)[c]	(0.1437)[c]				(0.0092)[c]
		(0.503)[d]	(0.1476)[d]	(0.1476)[d]	(0.1450)[d]				
	(12,0)	0.97659	0.14641	0.14641	0.14639	119.352	119.468	119.468	0
		(0.97818)[b]							(0.0032)[b]
	(20,0)	1.61787	0.14629	0.14629	0.14628	119.771	119.808	119.808	0
		(1.604)[a]							
Armchair	(3,3)	0.43411	0.14738	0.14765	0.14738	116.616	117.696	116.616	0
		(0.421)[d]	(0.1467)[d]	(0.1475)[d]	(0.1467)[d]	119.190	119.350	119.190	0
	(6,6)	0.84520	0.14646	0.14649	0.14646				
		(0.838)[a]							
		(0.8354)[c]	(0.1440)[c]	(0.1441)[c]	(0.1440)[c]				(0.0052)[c]
	(10,10)	1.40077	0.14631	0.14631	0.14631	119.711	119.760	119.711	0
		(1.390)[a]							
		(1.3776)[c]	(0.1438)[c]	(0.1437)[c]	(0.1438)[c]				(0.0030)[c]
Chiral	(4,2)	0.44352	0.14737	0.14761	0.14731	116.461	117.686	117.021	0
	(9,3)	0.88085	0.14645	0.14646	0.14643	119.210	119.381	119.305	0
	(15,5)	1.45865	0.14630	0.14631	0.14630	119.721	119.774	119.750	0

[a][2].
[b][3].
[c][6].
[d][22].

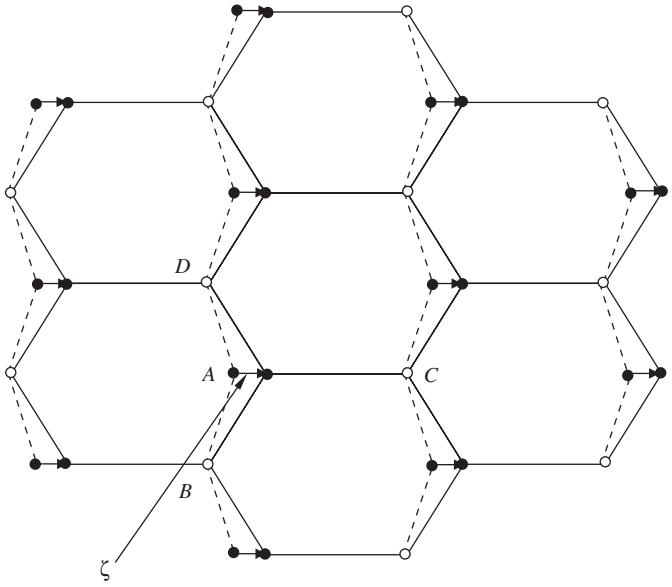

Fig. 2. The decomposition of a planar boron nitride nanotube (BNNT) "unrolled" from a deformed BNNT to two triangular sub-lattices composed of boron atoms and nitrogen atoms, respectively. There is a shift vector $\boldsymbol{\zeta}$ between two sub-lattices to ensure equilibrium of atoms. The solid and dashed lines denote the lattice structures with and without the shift vector $\boldsymbol{\zeta}$, respectively.

We use solid circles to denote boron atoms and open circles for nitrogen atoms. The hexagonal lattice can be decomposed into two triangular sub-lattices, one for boron atoms (solid circles) and the other for nitrogen atoms (open circles). Each triangular sub-lattice possesses centrosymmetry such that atoms within each sub-lattice follow the Cauchy—Born rule. For example, the length between two nitrogen atoms B and C on the "unrolled" plane for the deformed BNNT is obtained from (16) as

$$r_{BC}(\boldsymbol{E}) = \sqrt{\boldsymbol{r}_{BC}\cdot\boldsymbol{r}_{BC}} = \sqrt{\boldsymbol{r}_{BC}^{(0)}\cdot(\boldsymbol{I}+2\boldsymbol{E})\cdot\boldsymbol{r}_{BC}^{(0)}}, \tag{17}$$

where the dependence on the Green strain $\boldsymbol{E}$ is explicitly shown.

It is important to note, however, the solid-circle (boron) sub-lattice may undergo a shift vector $\boldsymbol{\zeta}$ with respect to the open-circle (nitrogen) sub-lattice as shown in Fig. 2, to relax atom positions in the hexagonal lattice in order to ensure equilibrium of atoms. We take the representative boron atom A and its three nearest-neighbor nitrogen atoms B, C and D to illustrate this. On top of the motion associated with the Cauchy—Born rule, the atom A is relaxed and moves additional $\boldsymbol{\zeta}$ relative to atoms B, C and D such that the lengths AB, AC and AD are readjusted to ensure equilibrium of atom A. The vector $\boldsymbol{r}_{AB}$ in Fig. 2 is the sum of $\boldsymbol{F}\cdot\boldsymbol{r}_{AB}^{(0)}$ (Cauchy—Born rule) and the shift vector $\boldsymbol{\zeta}$

$$\boldsymbol{r}_{AB} = \boldsymbol{F}\cdot\boldsymbol{r}_{AB}^{(0)} + \boldsymbol{\zeta}. \tag{18}$$

Without losing generality, we may write $\boldsymbol{\zeta} = \boldsymbol{F}\cdot\boldsymbol{\xi}$, where $\boldsymbol{\xi} = \boldsymbol{F}^{-1}\cdot\boldsymbol{\zeta}$ is an internal degree of freedom. The length of AB is then given in terms of Green strain $\boldsymbol{E}$ and the internal

degree of freedom ξ by

$$r_{AB}(\boldsymbol{E},\xi)=\sqrt{\boldsymbol{r}_{AB}\cdot\boldsymbol{r}_{AB}}=\sqrt{\left(\boldsymbol{r}_{AB}^{(0)}+\xi\right)\cdot(\boldsymbol{I}+2\boldsymbol{E})\cdot\left(\boldsymbol{r}_{AB}^{(0)}+\xi\right)}, \tag{19}$$

where the dependence on the Green strain $\boldsymbol{E}$ and internal degree of freedom ξ is explicitly shown.

Similar to (6)–(13) in Section 3.1, the bond length in the cylindrical configuration of a deformed BNNT can be obtained in terms of $\boldsymbol{E}$ and ξ via the lengths in (18) and (19).

3.3. Continuum strain energy density

The energy stored in an atomic bond AB, denoted by $V(r_{AB};\theta_{ABQ})$, is obtained from the multi-body interatomic potential in (1) once bond lengths and angles are known for the cylindrical configuration of deformed BNNT. The energy for each representative atom A is $\frac{1}{2}\left[V\left(r_{AB};\theta_{ABQ}\right)+V\left(r_{AC};\theta_{ACQ}\right)+V\left(r_{AD};\theta_{ADQ}\right)\right]$, where the factor 1/2 results from equal partition of energy between two atoms in the bond. The strain energy density W on the continuum level is the energy per unit area of the BNNT surface, and is related to the interatomic potential by

$$W(\boldsymbol{E},\xi)=\frac{V\left(r_{AB};\theta_{ABQ}\right)+V\left(r_{AC};\theta_{ACQ}\right)+V\left(r_{AD};\theta_{ADQ}\right)}{2\Omega_{\varepsilon}}, \tag{20}$$

where the dependence on the Green strain $\boldsymbol{E}$ and internal degree of freedom ξ is explicitly shown, and Ω_{ε} is the undeformed BNNT surface area per atom and is given by

$$\Omega_{\varepsilon}=\sqrt{s(s-a_1)(s-a_2)(s-a_3)} \tag{21}$$

with $s=(a_1+a_2+a_3)/2$.

The shift vector ζ introduced in Section 3.2 relaxes atom positions to ensure equilibrium of atoms. For a given Green strain $\boldsymbol{E}$, the shift vector ζ or the internal degree of freedom ξ is determined from equilibrium of atoms, which is equivalent to the minimization of strain energy density $\boldsymbol{W}(\boldsymbol{E},\xi)$ with respect to ξ, i.e.,

$$\frac{\partial W}{\partial\xi}=0. \tag{22}$$

This gives an implicit equation to determine ξ in terms of the Green strain $\boldsymbol{E}$, i.e., $\xi=\xi(\boldsymbol{E})$. It can be verified that $\xi=0$ for vanishing strain $\boldsymbol{E}=0$. The strain energy density is then written as $W=W[\boldsymbol{E},\xi(\boldsymbol{E})]$.

3.4. Stress and incremental modulus

The second Piola–Kirchhoff stress $\boldsymbol{T}$ is obtained from the total derivative of strain energy density W with respect to the Green strain $\boldsymbol{E}$,

$$\boldsymbol{T}=\frac{\mathrm{d}W}{\mathrm{d}\boldsymbol{E}}=\frac{\partial W}{\partial\boldsymbol{E}}+\frac{\partial W}{\partial\xi}\cdot\frac{\partial\xi}{\partial\boldsymbol{E}}=\frac{\partial W}{\partial\boldsymbol{E}}, \tag{23}$$

where $\partial W/\partial\xi=0$ has been used.

The stress increment $\dot{T}$ is related to the strain increment $\dot{\boldsymbol{E}}$ via the increment modulus tensor $\boldsymbol{C}$,

$$\dot{\boldsymbol{T}}=\boldsymbol{C}:\dot{\boldsymbol{E}}, \tag{24}$$

where $\boldsymbol{C}$ is the total derivative of $\boldsymbol{T}$ with respect to $\boldsymbol{E}$ given by

$$\boldsymbol{C}=\frac{\mathrm{d}\boldsymbol{T}}{\mathrm{d}\boldsymbol{E}}=\frac{\mathrm{d}}{\mathrm{d}\boldsymbol{E}}\left(\frac{\partial W}{\partial\boldsymbol{E}}\right)=\frac{\partial^2 W}{\partial\boldsymbol{E}\,\partial\boldsymbol{E}}-\frac{\partial^2 W}{\partial\boldsymbol{E}\,\partial\xi}\cdot\left(\frac{\partial^2 W}{\partial\xi\,\partial\xi}\right)^{-1}\cdot\frac{\partial^2 W}{\partial\xi\,\partial\boldsymbol{E}}. \tag{25}$$

Here we have used

$$\frac{\mathrm{d}\xi}{\mathrm{d}\boldsymbol{E}}=-\left(\frac{\partial^2 W}{\partial\xi\,\partial\xi}\right)^{-1}\cdot\left(\frac{\partial^2 W}{\partial\xi\,\partial\boldsymbol{E}}\right), \tag{26}$$

obtained from the derivative of $\partial W/\partial\xi=0$.

Eqs. (23) and (25) give the stress and incremental modulus in terms of strain and the interatomic potential. Such an approach to establish the constitutive model directly from interatomic potentials does not introduce any additional fitting parameters beyond those in interatomic potentials.

4. Young's modulus and stress–strain curve of boron-nitride nanotubes in simple tension

The Young's modulus of a single-wall BNNT along the axial direction Z can be obtained from the above incremental modulus tensor $\boldsymbol{C}$ at infinitesimal deformation ($\boldsymbol{E}=0$ and $\xi=0$) by $\left[C_{ZZZZ}-C_{ZZ\Theta\Theta}^2/(C_{\Theta\Theta\Theta\Theta})\right]_{E=0,\,\xi=0}$. Here the Young's modulus is in fact the elastic modulus multiplied by the tube thickness since the energy density in (20) is the energy per unit surface area of the BNNT. In order to avoid this ambiguity in thickness of single-wall BNNT, we normalize the Young's modulus of BNNT by its limit for a very large tube diameter, i.e., a flat sheet of boron and nitrogen atoms. Fig. 3 shows the normalized Young's modulus of BNNT vs. the tube diameter for armchair (n,n) and zigzag $(n,0)$ BNNTs. The normalized Young's moduli obtained from tight binding [2] and ab initio calculation [3] are also shown in Fig. 3, and they agree well with the present continuum analysis based on interatomic potentials. The Young's modulus becomes virtually independent of the nanotube diameter d_t once d_t exceeds 2 nm. This is because the B–N bond length (~0.15 nm) is much smaller than the nanotube diameter d_t for $d_t>2$ nm.

Fig. 4 shows the Young's modulus (without normalization) of BNNT vs. the nanotube diameter. For single-wall BNNTs, the thickness is taken as the monolayer thickness 0.34 nm of h-BN atomic structure. This is similar to the use of monolayer thickness 0.335 nm of graphite as the carbon nanotube thickness, though such an estimate is more suitable for multi-wall than single-wall nanotubes [29]. The Young's modulus given by the present continuum

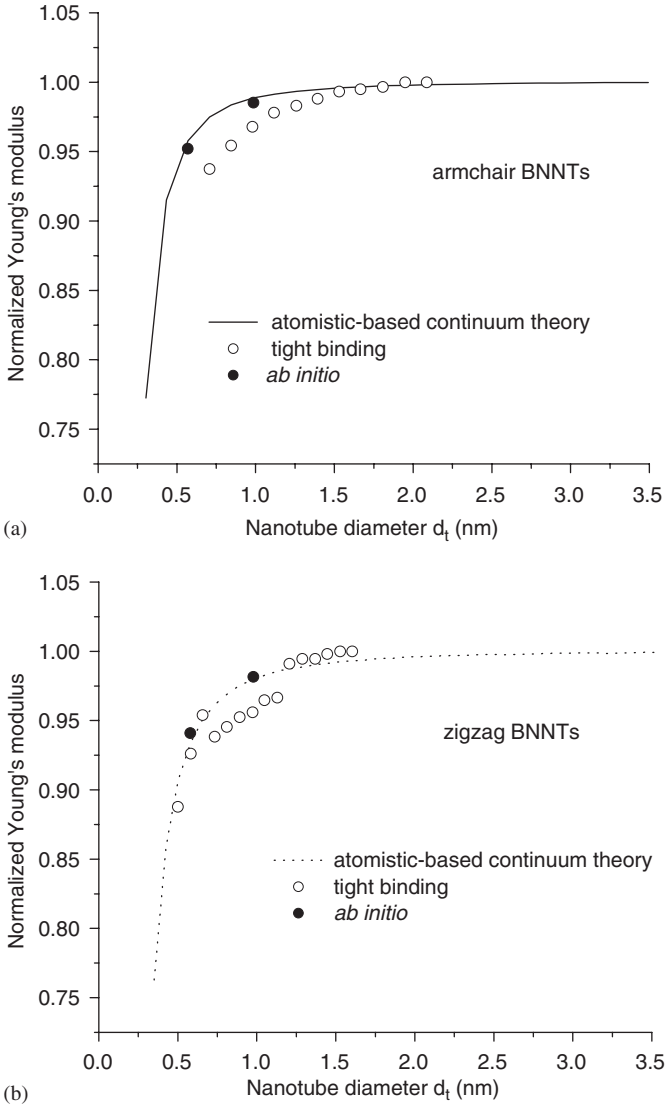

Fig. 3. Normalized Young's modulus of boron-nitride nanotubes (BNNTs) vs. the nanotube diameter for: (a) armchair BNNTs; and (b) zigzag BNNTs.

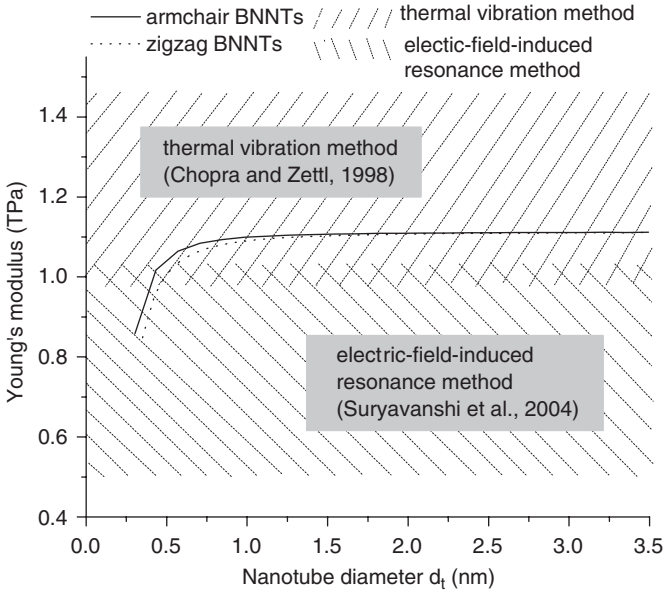

Fig. 4. The Young's modulus of boron-nitride nanotubes obtained from the atomistic-based continuum analysis and from two experiments.

analysis based on interatomic potentials ranges from 0.85 to 1.11TPa, depending on the BNNT diameter. Fig. 4 also shows the experimentally measured Young's modulus of multi-wall BNNTs, which ranges from 0.98 to 1.46TPa for the thermal vibration method [4] and from 0.505 to 1.031TPa for the electric-field-induced resonance method [5]. The Young's modulus predicted by the atomistic-based continuum analysis indeed falls into the range of experimental data, though the former is for single-wall BNNT and the latter are for multi-wall BNNTs.

The deformation in armchair and zigzag BNNTs subject to tension is axisymmetic and is characterized by the non-vanishing components $F_{\Theta\Theta}$ and F_{ZZ} of the deformation gradient. The non-zero components of Green strain are $E_{\Theta\Theta} = \frac{1}{2}(F_{\Theta\Theta}^2 - 1)$ and $E_{ZZ} = \frac{1}{2}(F_{ZZ}^2 - 1)$. The internal degree of freedom $\xi = \xi(E_{\Theta\Theta}, E_{ZZ})$ is determined from (22). The second Piola–Kirchhoff stress is then obtained in terms of $E_{\Theta\Theta}$ and E_{ZZ} from (23) as

$$T_{\Theta\Theta} = \frac{\partial W}{\partial E_{\Theta\Theta}} = 0, \tag{27}$$

$$T_{ZZ} = \frac{\partial W}{\partial E_{ZZ}}, \tag{28}$$

where (27) results from uniaxial tension and it is an implicit equation to determine $E_{\Theta\Theta}$ in terms of E_{ZZ}, i.e., $E_{\Theta\Theta} = E_{\Theta\Theta}(E_{ZZ})$. The non-zero components of incremental modulus $C_{\Theta\Theta\Theta\Theta}$, C_{ZZZZ}, $C_{\Theta\Theta ZZ} = C_{ZZ\Theta\Theta}$ and $C_{\Theta Z\Theta Z}$ are obtained from (25).

For a given axial strain E_{ZZ}, the axial force P on the BNNT can be obtained by integrating the normal stress traction $\boldsymbol{e}_Z \cdot (\boldsymbol{F} \cdot \boldsymbol{T} \cdot \boldsymbol{e}_Z)$ over the cross-section, which gives

$$P = \pi d_t F_{ZZ} T_{ZZ} = \pi d_t \sqrt{1 + 2E_{ZZ}}\, T_{ZZ}, \tag{29}$$

where d_t is the BNNT diameter prior to deformation, and T_{ZZ} is obtained from (28). Fig. 5 shows the axial force P, normalized by the BNNT radius $d_t/2$ prior to deformation, vs. the axial strain E_{ZZ} for four zigzag BNNTs $[(7,0),(10,0),(14,0),(\infty,0)]$ and four armchair BNNTs $[(4,4),(5,5),(8,8),(\infty,\infty)]$. For armchair BNNTs, the force–strain curve has very little dependence on the nanotube diameter since all curves for armchair BNNTs are very close. This also holds for zigzag BNNTs. However, the curves for armchair BNNTs are appreciably higher than those for zigzag BNNTs, which suggests that armchair BNNTs have higher resistance against tension than zigzag BNNTs. Similar observation have been made in carbon nanotubes [15]. Therefore, the effect of BNNT

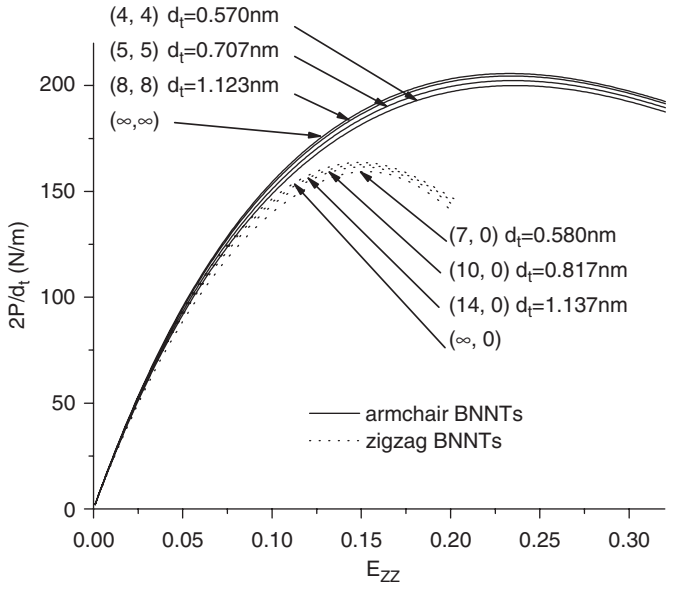

Fig. 5. The axial force P, normalized by the nanotube radius $d_t/2$ prior to deformation, vs. the axial strain E_{ZZ} for several armchair and zigzag boron-nitride nanotubes subject to simple tension.

diameter is secondary as compared to BNNT helicity (orientation).

5. Equilibrium equation

The equilibrium equation, in general, is

$$(\boldsymbol{F}\cdot\boldsymbol{T})\cdot\nabla=0, \tag{30}$$

where $\boldsymbol{F}$ is the deformation gradient, $\boldsymbol{T}$ is the second Piola–Kirchhoff stress, and ∇ is the gradient in the reference (undeformed) configuration, and it takes the form

$$\nabla=\boldsymbol{e}_R\frac{\partial}{\partial R}+\frac{\boldsymbol{e}_\Theta}{R}\frac{\partial}{\partial\Theta}+\boldsymbol{e}_Z\frac{\partial}{\partial Z}$$

in the cylindrical coordinate (R,Θ,Z) for the BNNT. The traction-free boundary condition on the surface of BNNT is

$$\boldsymbol{F}\cdot\boldsymbol{T}\cdot\boldsymbol{e}_R=0. \tag{31}$$

Integration of (30) over the vanishing thickness of BNNT, in conjunction with the boundary condition (31), gives the following equilibrium equations for a single-wall BNNT

$$\frac{1}{R}\frac{\partial}{\partial\Theta}(\boldsymbol{F}\cdot\boldsymbol{T})_{R\Theta}-\frac{1}{R}(\boldsymbol{F}\cdot\boldsymbol{T})_{\Theta\Theta}+\frac{\partial}{\partial Z}(\boldsymbol{F}\cdot\boldsymbol{T})_{RZ}=0, \tag{32a}$$

$$\frac{1}{R}(\boldsymbol{F}\cdot\boldsymbol{T})_{R\Theta}+\frac{1}{R}\frac{\partial}{\partial\Theta}(\boldsymbol{F}\cdot\boldsymbol{T})_{\Theta\Theta}+\frac{\partial}{\partial Z}(\boldsymbol{F}\cdot\boldsymbol{T})_{\Theta Z}=0, \tag{32b}$$

$$\frac{1}{R}\frac{\partial}{\partial\Theta}(\boldsymbol{F}\cdot\boldsymbol{T})_{Z\Theta}+\frac{\partial}{\partial Z}(\boldsymbol{F}\cdot\boldsymbol{T})_{ZZ}=0, \tag{32c}$$

where R is the BNNT radius in the undeformed configuration, $\boldsymbol{T}$ is the second Piola–Kirchhoff stress averaged over the BNNT thickness, and its non-vanishing components are $T_{\Theta\Theta}$, T_{ZZ}, and $T_{Z\Theta}$.

6. Bifurcation analysis for single-wall boron-nitride nanotubes

We use the atomistic-based constitutive model to investigate the deformation of armchair and zigzag single-wall BNNTs subject to tension. For relatively small applied strain, the deformation in the BNNT is uniform, and the stress–strain curve is given in Section 4. Once the applied strain exceeds a critical value, non-uniform deformation begins in the BNNT. This is called bifurcation, and is similar to necking in a tensile bar.

The bifurcation analysis for BNNTs in this section is similar to [30] for carbon nanotubes. Let $\boldsymbol{U}$ denote the displacement, which is related to the deformation gradient $\boldsymbol{F}$ by $\boldsymbol{F}=\boldsymbol{I}+\boldsymbol{U}\nabla$. At the onset of bifurcation, the deformation gradient, stress and strain are still uniform, but their increments begin to be non-uniform and may depend on Θ and Z. The non-uniform increment of deformation gradient $\dot{\boldsymbol{F}}$ is given in terms of the displacement increment $\dot{\boldsymbol{U}}$ by

$$\begin{aligned}
&\dot F_{R\Theta}=\frac{1}{R}\frac{\partial\dot U_R}{\partial\Theta}-\frac{\dot U_\Theta}{R},\quad \dot F_{\Theta\Theta}=\frac{\dot U_R}{R}+\frac{1}{R}\frac{\partial\dot U_\Theta}{\partial\Theta},\\
&\dot F_{Z\Theta}=\frac{1}{R}\frac{\partial\dot U_Z}{\partial\Theta},\quad \dot F_{RZ}=\frac{\partial\dot U_R}{\partial Z},\quad \dot F_{\Theta Z}=\frac{\partial\dot U_\Theta}{\partial Z},\\
&\dot F_{ZZ}=\frac{\partial\dot U_Z}{\partial Z},
\end{aligned} \tag{33}$$

where only components within the tube surface are given. The corresponding non-zero components of Green strain $\dot{\boldsymbol{E}}$ are

$$\begin{aligned}
&\dot E_{\Theta\Theta}=F_{\Theta\Theta}\dot F_{\Theta\Theta},\ \dot E_{ZZ}=F_{ZZ}\dot F_{ZZ},\\
&\dot E_{Z\Theta}=\dot E_{\Theta Z}=\tfrac{1}{2}\big(F_{\Theta\Theta}\dot F_{\Theta Z}+F_{ZZ}\dot F_{Z\Theta}\big),
\end{aligned} \tag{34}$$

where $F_{\Theta Z}=0$ at the onset of bifurcation has been used.

The non-vanishing components of stress increment are obtained from (24) as

$$\dot T_{\Theta\Theta}=C_{\Theta\Theta\Theta\Theta}\dot E_{\Theta\Theta}+C_{\Theta\Theta ZZ}\dot E_{ZZ}, \tag{35a}$$

$$\dot T_{ZZ}=C_{ZZ\Theta\Theta}\dot E_{\Theta\Theta}+C_{ZZZZ}\dot E_{ZZ}, \tag{35b}$$

$$\dot T_{\Theta Z}=\dot T_{Z\Theta}=2C_{\Theta Z\Theta Z}\dot E_{\Theta Z}. \tag{35c}$$

The substitution of (33)–(35) into the incremental form of equilibrium Eq. (32) gives

$$\begin{aligned}
&\left(T_{ZZ}\frac{\partial^2}{\partial Z^2}-\frac{1}{R^2}C_{\Theta\Theta\Theta\Theta}F_{\Theta\Theta}^2\right)\dot U_R-\frac{1}{R^2}C_{\Theta\Theta\Theta\Theta}F_{\Theta\Theta}^2\frac{\partial\dot U_\Theta}{\partial\Theta}\\
&\quad-\frac{1}{R}C_{\Theta\Theta ZZ}F_{\Theta\Theta}F_{ZZ}\frac{\partial\dot U_Z}{\partial Z}=0,
\end{aligned} \tag{36a}$$

$$\frac{1}{R^2}C_{\Theta\Theta\Theta\Theta}F_{\Theta\Theta}^2\frac{\partial\dot{U}_R}{\partial\Theta}+\left[\frac{1}{R^2}C_{\Theta\Theta\Theta\Theta}F_{\Theta\Theta}^2\frac{\partial^2}{\partial\Theta^2}+\left(T_{ZZ}+C_{\Theta Z\Theta Z}F_{\Theta\Theta}^2\right)\frac{\partial^2}{\partial Z^2}\right]\dot{U}_\Theta+\frac{1}{R}(C_{\Theta\Theta ZZ}+C_{\Theta Z\Theta Z})F_{\Theta\Theta}F_{ZZ}\frac{\partial^2\dot{U}_Z}{\partial\Theta\,\partial Z}=0, \tag{36b}$$

$$\frac{1}{R}C_{\Theta\Theta ZZ}F_{\Theta\Theta}F_{ZZ}\frac{\partial\dot{U}_R}{\partial Z}+\frac{1}{R}(C_{\Theta\Theta ZZ}+C_{\Theta Z\Theta Z})F_{\Theta\Theta}F_{ZZ}\frac{\partial^2\dot{U}_\Theta}{\partial\Theta\,\partial Z}+\left[\frac{1}{R^2}C_{\Theta Z\Theta Z}F_{ZZ}^2\frac{\partial^2}{\partial\Theta^2}+\left(T_{ZZ}+C_{ZZZZ}F_{ZZ}^2\right)\frac{\partial^2}{\partial Z^2}\right]\dot{U}_Z=0. \tag{36c}$$

The BNNT is subjected to axial displacement and vanishing shear stress tractions at the ends. Therefore, at the onset of bifurcation, the increments of axial displacement and shear stress tractions vanish at both ends. The increments of stress tractions at the ends of BNNT are given by $\frac{\mathrm{d}}{\mathrm{d}t}(\boldsymbol{F}\cdot\boldsymbol{T}\cdot\boldsymbol{e}_Z)=\dot{\boldsymbol{F}}\cdot\boldsymbol{T}\cdot\boldsymbol{e}_Z+\boldsymbol{F}\cdot\dot{\boldsymbol{T}}\cdot\boldsymbol{e}_Z$. The vanishing of increments of shear stress tractions then gives $\dot{F}_{RZ}T_{ZZ}=0$ and $\dot{F}_{\Theta Z}T_{ZZ}+F_{\Theta\Theta}\dot{T}_{\Theta Z}=0$ in the R- and Θ- directions, respectively. In conjunction with (33), the incremental boundary conditions at the two ends of BNNT can be written as

$$\dot{U}_Z=\frac{\partial\dot{U}_R}{\partial Z}=\frac{\partial\dot{U}_\Theta}{\partial Z}=0\quad\text{at } Z=0 \text{ and } L, \tag{37}$$

where L is the length of BNNT.

The homogeneous governing equations (36) and boundary conditions (37) constitute an eigenvalue problem for the displacement increment $\dot{\mathbf{U}}$. The eigenvalue is the axial strain E_{ZZ} (or equivalently, F_{ZZ}). In other words, (36) and (37) have only the trivial solution $\dot{\mathbf{U}}=0$ until the axial strain E_{ZZ} reaches a critical value $(E_{ZZ})_{critical}$ for bifurcation.

The general solution of (36), satisfying the homogeneous boundary condition (37), takes the form

$$\left[\dot{U}_R,\dot{U}_\Theta,\dot{U}_Z\right]=\left[\dot{U}_{Rm}^{(n)}\cos n\Theta\cos\frac{m\pi Z}{L},\ \dot{U}_{\Theta m}^{(n)}\sin n\Theta\cos\frac{m\pi Z}{L},\ \dot{U}_{Zm}^{(n)}\cos n\Theta\sin\frac{m\pi Z}{L}\right] \tag{38}$$

where $m=1,2,3,\ldots$ and $n=0,1,2,\ldots$ are the eigen mode numbers in the Z and Θ directions, respectively, and $\left[\dot{U}_{Rm}^{(n)},\dot{U}_{\Theta m}^{(n)},\dot{U}_{Zm}^{(n)}\right]$ is the eigenvector. The substitution of (38) into (36) yields three homogeneous, linear algebraic equations for $\dot{U}_{Rm}^{(n)}$, $\dot{U}_{\Theta m}^{(n)}$ and $\dot{U}_{Zm}^{(n)}$. In order to have a non-trivial solution, the determinant of 3×3 coefficient matrix for the linear algebraic equations must vanish, which gives the following critical condition for bifurcation:

$$\left(C_{ZZZZ}+\frac{T_{ZZ}}{F_{ZZ}^2}\right)\left[C_{\Theta\Theta\Theta\Theta}+\frac{T_{ZZ}}{F_{\Theta\Theta}^2}\left(\frac{m\pi R}{L}\right)^2\right]-C_{\Theta\Theta ZZ}^2+\frac{n^2T_{ZZ}}{T_{ZZ}+C_{\Theta Z\Theta Z}F_{\Theta\Theta}^2}\left[C_{\Theta\Theta\Theta\Theta}\left(C_{ZZZZ}+\frac{T_{ZZ}}{F_{ZZ}^2}\right)-(C_{\Theta\Theta ZZ}+C_{\Theta Z\Theta Z})^2+C_{\Theta Z\Theta Z}\left(C_{\Theta Z\Theta Z}+\frac{T_{ZZ}}{F_{\Theta\Theta}^2}\right)+(n^2+1)C_{\Theta\Theta\Theta\Theta}C_{\Theta Z\Theta Z}\left(\frac{L}{m\pi R}\right)^2\right] \tag{39}$$

The above equation, in conjunction with the uniaxial condition $T_{\Theta\Theta}=0$ in (27), provides two equations to determine $E_{\Theta\Theta}$ and E_{ZZ} (or equivalently $F_{\Theta\Theta}$ and F_{ZZ}) at the onset of bifurcation. The strains thus obtained depend on the eigen mode numbers m and n. The numerical results show that the axial strain E_{ZZ} for $m=1$ and $n=0$ is always the minimum among all E_{ZZ} for $m=1,2,3\ldots$ and $n=0,1,2,\ldots$. The axial strain for $m=1$ and $n=0$ at bifurcation is denoted by $(E_{ZZ})_{critical}$, and the corresponding bifurcation mode is axisymmetric ($n=0$).

The critical condition for bifurcation is then obtained from (39) by letting $m=1$ and $n=0$, i.e.,

$$\left(C_{ZZZZ}+\frac{T_{ZZ}}{F_{ZZ}^2}\right)\left[C_{\Theta\Theta\Theta\Theta}+\frac{T_{ZZ}}{F_{\Theta\Theta}^2}\left(\frac{\pi R}{L}\right)^2\right]-C_{\Theta\Theta ZZ}^2=0. \tag{40}$$

Fig. 6 shows the bifurcation strain $(E_{ZZ})_{\text{critical}}$ vs. the aspect ratio d_t/L for several armchair and zigzag BNNTs, where d_t and L are the nanotube diameter and length, respectively. It is observed that the bifurcation strain is virtually independent of the nanotube aspect ratio d_t/L since all curves in Fig. 6 are very flat.

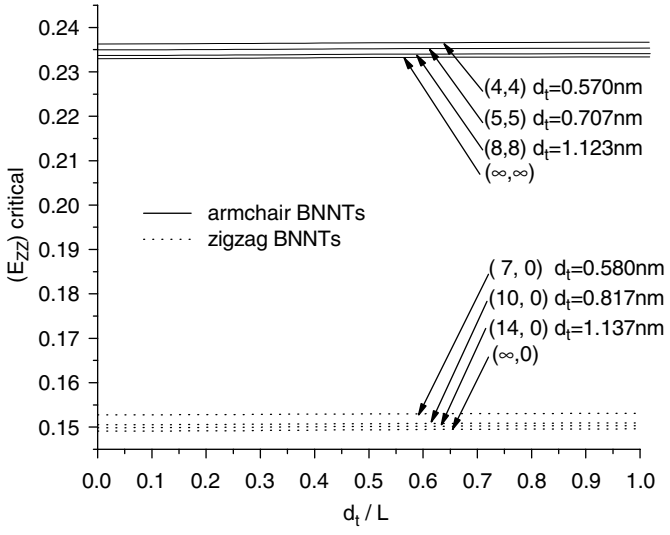

Fig. 6. The bifurcation strain vs. the diameter/length ratio for several armchair and zigzag boron-nitride nanotubes.

Furthermore, the bifurcation strain depends rather weakly on the nanotube diameter d_t. For example, for armchair BNNTs, the bifurcation strain ranges from 0.233 to 0.236 for tube diameter from ∞ to 0.570 nm. For zigzag BNNTs, the variation of $(E_{ZZ})_{critical}$ is also small, from 0.149 to 0.153 for tube diameter from ∞ to 0.580nm. However, the bifurcation strain depends strongly on the helicity of BNNTs. With approximately the same diameter, the bifurcation strain for the (4,4) armchair BNNT is more than 50% higher than that for the (7,0) zigzag BNNT.

7. Concluding remarks

We have proposed an atomistic-based continuum theory for boron-nitride nanotubes (BNNTs) based on interatomic potentials for boron and nitrogen. The theory is established from the modified Cauchy–Born rule to link the continuum constitutive model for BNNTs to interatomic potentials of boron and nitrogen. It is shown that the BNNT helicity (e.g., armchair vs. zigzag) has a strong influence on the mechanical behavior of BNNT under tension, but the BNNT radius has little effect. We have applied the atomistic-based continuum theory to study the Young's modulus, stress–strain curve and onset of bifurcation in single-wall BNNTs under tension. Here the onset of bifurcation indicates the beginning of non-uniform deformation in BNNTs subject to uniform tension, and is similar to necking in a tensile bar. The bifurcation strain is approximately independent of the BNNT radius and length, but depends strongly on the BNNT helicity. It is about 23% for armchair BNNTs, and 15% for zigzag BNNTs.

Acknowledgements

Y.H. acknowledges the support from NSF (Grants 00-99909, 01-03257, and 03-28162 via the Nano-CEMMS Center at UIUC), Office of Naval Research (Grant N00014-01-1-0205, Program Manager Dr. Y. D. S. Rajapakse), and NSFC. K.C.H. acknowledges support from NSFC and the Ministry of Education, China.

References

[1] Tang CC, Bando Y, Sato T, Kurashima K. A novel precursor for synthesis of pure boron nitride nanotubes. Chemical Communications 2002;12:1290–1.

[2] Hernández E, Goze C, Bernier P, Rubio A. Elastic properties of C and B*x*C*y*N*z* composite nanotubes. Physical Review Letters 1998;80:4502–5.

[3] Kudin KN, Scuseria GE, Yakoboson BI. C_2F, BN, and C nanoshell elasticity from *ab initio* computations. Physical Review B 2001;64:235406.

[4] Chopra NG, Zettl A. Measurement of the elastic modulus of a multi-wall boron nitride nanotube. Solid State Communications 1998;105:297–300.

[5] Suryavanshi AP, Yu MF, Wen JG, Tang CC, Bando Y. Elastic modulus and resonance behavior of boron nitride nanotubes. Applied Physics Letters 2004;84:2527–9.

[6] Akdim B, Pachter R, Duan XF, Adams WW. Comparative theoretical study of single-wall carbon and boron-nitride nanotubes. Physical Review B 2003;67:245404.

[7] Bettinger HF, Dumitrică T, Scuseria GE, Yakobson BI. Mechanically induced defects and strength of BN nanotubes. Physical Review B 2002;65:041406.

[8] Dumitrică T, Bettinger HF, Scuseria GE, Yakobson BI. Thermodynamics of yield in boron nitride nanotubes. Physical Review B 2003;68:085412.

[9] Hernández E, Goze C, Bernier P, Rubio A. Elastic properties of single-wall nanotubes. Applied Physics A-Materials Science & Processing 1999;68:287–92.

[10] Moon WH, Hwang HJ. Molecular-dynamics simulation of structure and thermal behavior of boron nitride nanotubes. Nanotechnology 2004;15:431–4.

[11] Vaccarini L, Goze C, Henrard L, Hernández E, Bernier P, Rubio A. Mechanical and electronic properties of carbon and boron-nitride nanotubes. Carbon 2000;38:1681–90.

[12] Albe K, Möller W. Modelling of boron nitride: atomic scale simulations on thin film growth. Computational Materials Science 1998;10:111–5.

[13] Albe K, Möller W, Heinig KH. Computer simulation and boron nitride. Radiation Effects and Defects in Solids 1997;141:85–97.

[14] Zhang P, Huang Y, Geubelle PH, Hwang KC. On the continuum modeling of carbon nanotubes. Acta Mechanica Sinica 2002;18:528–36.

[15] Jiang H, Zhang P, Liu B, Huang Y, Geubelle PH, Gao H, et al. The effect of nanotube radius on constitutive model for cabon nanotubes. Computaional Materials Science 2003;28:429–42.

[16] Albe K. Theoretical study of boron nitride modifications at hydrostatic pressures. Physical Review B 1997;55:6203.

[17] Furthmüller J, Hafner J, Kresse G. *Ab initio* calculation of the structural and electronic properties of carbon and boron nitride using ultrasoft pseudopotentials. Physical Review B 1994;50:15606.

[18] Janotti A, Wei SH, Singh DJ. First-principles study of the stability of BN and C. Physical Review B 2001;64:174107.

[19] Koga H, Nakamura Y, Watanabe S, Yoshida T. Molecular dynamics study of the role of ion bombardment in cubic boron nitride thin film deposition. Surface and Coatings Technology 2001;142–144:911–5.

[20] Sibona GJ, Schreiber S, Hoppe RHW, Stritzker B, Revnic A. Numerical simulation of production processes of layered materials. Materials Science in Semiconductor Processing 2003;6:71–6.

[21] Moon WH, Hwang HJ. Molecular-dynamics simulation of defect formation energy in boron nitride nanotubes. Physics Letters A 2004;320:446–51.

[22] Xu H, Ma J, Chen X, Hu Z, Huo K, Chen Y. The electronic structure and formation mechanisms of the single-walled BN nanotube with small diameter. The International Journal of Physical Chemistry B 2004;108:4024–34.

[23] Born M, Huang K. Dynamical Theory of the Crystal Lattices. Oxford: Oxford University Press; 1954.

[24] Milstein F. Review: theoretical elastic behavior at large strains. Journal of Material Science 1980;15:1071–84.

[25] Arroyo M, Belytschko T. An atomistic-based finite deformation membrane for single layer crystalline films. Journal of the Mechanics and Physics of Solids 2002;50:1941–77.

[26] Tadmor EB, Smith GS, Bernstein N, Kaxiras E. Mixed finite element and atomistic formulation for complex crystals. Physical Review B 1999;59:235–45.

[27] Weiner JH. Statistical mechanics of elasticity. New York: Wiley; 1983.

[28] Zhang P, Huang Y, Gao H, Hwang KC. Fracture nucleation in single-wall carbon nanotubes under tension: a continuum analysis incorporating interatomic potentials. Journal of Applied Mechanics—Transactions of the ASME 2002;69:454–8.

[29] Yakobson BI, Avouris P. Mechanical properties of carbon nanotubes. In: Dresselhaus MS, Dresselhaus G, Avouris P, editors. Carbon Nanotubes. vol. 80 of Topics in Applied Physics. p. 287–329.
[30] Zhang P, Jiang H, Huang Y, Geubelle PH, Hwang KC. An atomistic-based continuum theory for carbon nanotubes: analysis of fracture nucleation. Journal of the Mechanics and Physics of Solids 2004;52:977–98.
[33] Zhang P, Huang Y, Geubelle PH, Klein PA, Hwang KC. The elastic modulus of single-wall carbon nanotubes: a continuum analysis incorporating interatomic potentials. International Journal of Solids and Structures 2002;39:3893–906.